

Parameter estimation for Euler equations with uncertain inputs

Sergiy Zhuk

Tigran Tchraikian

Abstract—The paper presents a new state estimation algorithm for 2D incompressible Euler equations with periodic boundary conditions and uncertain but bounded inputs and initial conditions. The algorithm converges (in L^2 -sense) to a least squares estimator given incomplete and noisy observations. It is also shown experimentally that the proposed algorithm applies to several conservation laws developing shock discontinuities. The results are illustrated by numerical examples.

I. INTRODUCTION

Data assimilation algorithms represent a backbone of modern cyber-physical systems. These algorithms allow one to optimally combine *a priori* knowledge encoded in equations of mathematical physics with *a posteriori* information in the form of sensor readings. Weather forecasting is one of many examples where data assimilation is applied to improve predictions generated by hydrodynamical models. The divergence-free Euler equations provide the most basic model of incompressible flows of homogeneous inviscid fluids [7], yet this model may provide insights in studies of turbulence. We refer the reader to [2] for a detailed overview of various mathematical questions related to Euler equations.

In this paper we design a new state estimator for 2D Euler equations subject to uncertain but bounded input and unknown initial conditions. We rely on a vorticity-stream formulation of the Euler equations. The resulting vorticity equation describes the rotation of the vorticity of the fluid velocity field (see Section II). We stress that the homogenous vorticity equation possesses a nice property: the L^2 -norm of the vorticity is conserved over time. The latter, in fact, allows one to prove existence and uniqueness

of the solution of 2D Euler equations globally (in time) [7, Cor.3.3, p.116]. Assuming periodic boundary conditions, we apply Fourier-Galerkin (FG) approximation: we project the vorticity equation onto a subspace generated by $\{e^{inx}\}_{|n|\leq N}$ and obtain an ODE for the projection coefficients, a FG model. Note that Fourier-Galerkin approximation possesses a spectral convergence rate provided the solution of the Euler equation is smooth [1]. Although the main results of this work may be derived for the case of bounded domains with non-penetration boundary conditions or unbounded domains (\mathbb{R}^2), we focus on smooth periodic flows to simplify the convergence analysis. We refer the reader to Section II, where other types of boundary conditions and weak solutions of Euler equations are discussed.

Given an ODE representing projection coefficients, we design a discrete-in-time FG model such that the L^2 -norm of the discrete vorticity is conserved over time (see Section III-B). This property allows us to prove the convergence of the approximations provided by the discrete FG model to a solution of the continuous FG model. We then derive the state estimator (in the form of a minimax filter) for the discrete FG model and note that the combination of the mentioned convergence proof with results of [6] may be used to derive a continuous formulation of the minimax filter (see Section III-C). To the best of our knowledge, this result is new. A similar approach has been used to design data assimilation algorithms for scalar macroscopic traffic flow models [9] and flood models (StVenant equations) [11]. We stress that the proposed method shows very good performance not only for smooth periodic flows but also for conservation laws with shock discontinuities and non-periodic boundary conditions (see Section IV).

Data assimilation for systems of hyperbolic conservation laws based on the calculus of variations

was proposed in [3], where the authors adopt the strategy: “optimize”, then “discretize” so that the estimate of the initial density does not depend on a discretization method. In contrast, the present paper solves the filtering problem; that is, the state estimate at time instant, t , depends on the observation at the same time instant and the previous estimate only. A comparison of classical filtering algorithms (extended Kalman filter and ensemble Kalman filter) for scalar conservation laws with quadratic non-linearity may be found in [4]. Adaptive parameter estimators for hyperbolic equations were considered for instance in [5].

This paper is organized as follows. The next section presents a brief overview of Euler equations. Section II-A presents discrete in time FG model for Euler equations; the state estimation algorithm is shown in section III-C. Numerical experiments are given in section IV. Section V contains concluding remarks.

Notation. Let Ω denote a subset of \mathbb{R}^2 with boundary $\partial\Omega$, and \vec{n} is a normal vector for $\partial\Omega$ pointing outside, $\Omega_T := \Omega \times [0, T]$. $C^s(\Omega)$ denotes a space of continuously differentiable functions on Ω (up to order s), $L^2(\Omega)$ is the space of square-integrable functions on Ω , $H^1(\Omega)$ is a Sobolev space of functions with weak derivatives of $L^2(\Omega)$ -class. $\text{div}(\vec{u}) = \partial_{x_1} u_1 + \partial_{x_2} u_2$, $\text{curl}(\vec{u}) = \partial_{x_1} u_2 - \partial_{x_2} u_1$, $\nabla u = (\partial_{x_1} u, \partial_{x_2} u)^\top$, $\nabla^\perp u = (-\partial_{x_2} u, \partial_{x_1} u)^\top$. $\vec{u} \cdot \vec{v}$ denotes the canonical inner product of \mathbb{R}^2 , $H^2 := H \times H$ denotes the cartesian product of H with itself. $L^2(t_0, t_1, H) := \{f : f(t) \in H \text{ and } \int_0^T \|f(t)\|_H^2 dt < +\infty\}$. We write $u = v$ a.e. on Ω if $u(x) = v(x)$ for almost all $x \in \Omega$.

II. EULER EQUATIONS

Assume that ω verifies the vorticity-stream formulation of the Euler equation:

$$\begin{aligned} \partial_t \omega + \vec{u} \cdot \nabla \omega &= f, & -\Delta \psi &= \omega, \\ \vec{u} &= \bar{u} + \nabla^\perp \psi, & \omega(0) &= \text{curl}(\vec{u}_0), \\ (x, t) &\in \Omega_T := [-r, r]^2 \times [0, T], \end{aligned} \quad (1)$$

where $\bar{u} \in \mathbb{R}^2$ is a given vector, $\vec{u}_0 \in C^2(\Omega)^2$ is a smooth 1-periodic vector-function and $f \in C^1(\Omega_T)$ has zero mean, $\int_\Omega f(x, t) dx = 0$. It is not hard to prove (see [7, Prop 2.4, p.50]) that $\vec{u} = (u_1, u_2)^\top \in C^2(\Omega_T)^2$ is a smooth 1-periodic solution of the incompressible Euler equation on Ω_T :

$$\begin{aligned} \frac{d\vec{u}}{dt} + (\vec{u} \cdot \nabla) \vec{u} + \nabla p &= \vec{f}, \\ \text{div}(\vec{u}) &= 0, \vec{u}(0) = \vec{u}_0 + \bar{u}, \end{aligned} \quad (2)$$

where $\vec{f} \in C^2(\Omega_T)$ and $\text{curl}(\vec{f}) = f$, and the pressure p is a function of \vec{u} and \vec{f} .

We note that Euler equation (2) has the unique smooth solution \vec{u} for $\Omega = \mathbb{R}^2$ provided $\vec{f} = 0$ and \vec{u}_0 is a smooth function such that $\text{div}(\vec{u}_0) = 0$ and $\text{curl}(\vec{u}_0) \in L^1(\mathbb{R}^2)$ (see [7, L.3.2, p.93 and Cor.3.3, p.116]). For the case of bounded domains with smooth boundary one may also derive existence of smooth solutions for (2) provided \vec{u}_0 and \vec{f} are smooth and $\vec{u}_0 \cdot \vec{n} = 0$ on $\partial\Omega$ (see [10, p.356]). Weak solutions (or Sobolev space solutions) for (2) were constructed in [12] provided $|\text{curl}(\vec{u}_0)|$ is bounded, and $\vec{f} \in C(0, T, L^p(\Omega))$ is so that $|\text{curl}(\vec{f})|$ is bounded. Solutions of $L^2(0, T, L^2(\mathbb{R}^2)^2)$ -class corresponding to so called vortex sheets were discussed in [7, p.303].

A. Fourier-Galerkin approximation

Define

$$b(\vec{u}, w, v) := \int_\Omega (\vec{u} \cdot \nabla w) v dx.$$

Assume that $\text{div}(\vec{u}) = 0$ and \vec{u}, w, v are smooth 1-periodic functions on Ω . We find integrating by parts:

$$b(\vec{u}, w, v) = -b(\vec{u}, v, w). \quad (3)$$

Now, we apply Fourier spectral method to construct a finite dimensional approximation of (1). Let $s \in \mathbb{Z}^2$ and define $\phi_s(x) := \frac{e^{i\pi r^{-1} s \cdot x}}{2r}$. It is known that $\{\phi_s\}_{s \in \mathbb{Z}^2}$ is a total orthonormal system in $L^2(\Omega)$ and $(\phi_s, \phi_k)_{L^2(\Omega)} = \delta_{s_1, k_1} \delta_{s_2, k_2}$ where s_i, k_i are components of s, k . Now, we multiply (1) by ϕ_s

and integrate over Ω . We obtain a weak vorticity formulation:

$$\frac{d}{dt}(\omega, \phi_s)_{L^2(\Omega)} + b(\vec{u}, \omega, \phi_s) = (f, \phi_s)_{L^2(\Omega)}.$$

Let us now set $\omega^N(x, t) := \sum_{|k_i| \leq N} \omega_k(t) \phi_k(x)$ with $\omega_k(t) := (\omega(t), \phi_k)_{L^2(\Omega)}$ and plug ω^N into the above formulation. We get the following ODE for the coefficients:

$$\dot{\omega}_s + \sum_{|k_i| \leq N} b(\vec{u}, \phi_k, \phi_s) \omega_k(t) = (f, \phi_s)_{L^2(\Omega)}.$$

Define $\vec{\omega}(t) := \{\omega_s(t)\}_{|s_{1,2}| \leq N}$, $\vec{f}(t) := \{(f(t), \phi_s)_{L^2(\Omega)}\}_{|s_{1,2}| \leq N}$ and set

$$B(\vec{\omega}) := \{b(\vec{u}, \phi_k, \phi_s)\}_{|s_{1,2}|, |k_{1,2}| \leq N}.$$

Now we use this notation to rewrite the finite dimensional vorticity formulation in the vector form: $\frac{d\vec{\omega}}{dt} + B(\vec{\omega})\vec{\omega} = \vec{f}$ with initial condition $\vec{\omega}(0) = \vec{\omega}_0$ where $\vec{\omega}_0 := \{\omega_s(0)\}_{|s_{1,2}| \leq N}$. We stress that $B(\vec{\omega}) = -B^\top(\vec{\omega})$ as $b(\vec{u}, \phi_k, \phi_s) = -b(\vec{u}, \phi_s, \phi_k)$ by (3) so that $B(\vec{\omega})$ is skew-symmetric.

III. MAIN RESULTS

A. Problem statement

Let $\vec{\omega}$ solve

$$\frac{d\vec{\omega}}{dt} + B(\vec{\omega})\vec{\omega} = \vec{f}, \quad \vec{\omega}(0) = \vec{\omega}_0, \quad (4)$$

and assume that a vector-function $\vec{\gamma}$ is observed in the following form ($|k_{1,2}| \leq M$):

$$\vec{\gamma}_k(t) = \sum_{|s_{1,2}| \leq N} (H_k, \phi_s)_{L^2(\Omega)} \omega_s(t) + \eta_k(t), \quad (5)$$

where $H_k \in L^2(\Omega)$ and $\vec{\eta} = \{\eta_k\}_{|k_{1,2}| \leq M}$ is a measurable vector-function modelling noise. Our aim is to construct a state estimate $\hat{\omega}(T)$ for $\vec{\omega}(T)$ given data $\vec{\gamma}$ and assuming that

$$\vec{\omega}_0^\top S \vec{\omega}_0 + \int_0^T \vec{f}^\top Q \vec{f} + \vec{\eta}^\top R \vec{\eta} dt \leq 1 \quad (6)$$

provided S, Q, R are symmetric positive definite matrices of appropriate dimensions.

Let us stress that if $\vec{\omega}$ is the solution of (4), ω^N corresponds¹ to $\vec{\omega}$ and ω solves (1) then according to [1, T.5.1] we have:

$$\begin{aligned} \|\omega^N(\cdot, t) - \omega(\cdot, t)\|_{L^2(\Omega)} &\leq e^{g(t)} N^{-2l} \|\omega(\cdot, 0)\|_{H^l(\Omega)}^2 \\ &+ e^{g(t)} N^{2-l} \max_{0 \leq \tau \leq t} \|\omega(\cdot, \tau)\|_{H^l(\Omega)}, \quad g(t) \geq 0. \end{aligned} \quad (7)$$

This so called spectral convergence rate justifies our choice of the state equation. Namely, (4) is a standard finite dimensional Fourier-Galerkin model with uncertain input \vec{f} . Now, following the idea of [14], [15] we may incorporate the effect of the unresolved modes (the projection error) by simply adding another model error term e and introduce an additional algebraic equation to filter out inadmissible e (see [8], [13]) so that the exact projection coefficients of ω will be among the solutions of (4). On the other hand, the above convergence rate estimate suggests that the effect of e is negligible for reasonably large N and l (so for smooth ω) and it may be therefore absorbed by \vec{f} (by increasing the size of the ellipsoid (6)).

B. Discrete Fourier-Galerkin model

Assume $f = 0$. If we multiply (1) by ω and integrate over Ω we get: $\frac{1}{2} \partial_t \|\omega\|_{L^2(\Omega)}^2 = (f, \omega)_{L^2(\Omega)}$ as $b(\vec{u}, \omega, \omega) = 0$ by (3). Hence, $L^2(\Omega)$ -norm of ω is conserved. We stress that (4) has the same property, namely $\|\vec{\omega}\|_{\mathbb{R}^{2N+1}}^2$ is conserved as $B(\vec{\omega})$ is skew-symmetric. In what follows we propose a method which approximates $\vec{\omega}(jh)$ by $\tilde{\omega}_j := \tilde{\omega}(jh)$, $j = \overline{0, m}$, $h := \frac{T}{m}$, $m \in \mathbb{N}$ and the norm of $\tilde{\omega}_j$ is conserved.

By Newton-Leibniz formula we get:

$$\vec{\omega}((j+1)h) = \vec{\omega}(jh) - \int_{jh}^{(j+1)h} B(\vec{\omega}(\tau)) \vec{\omega}(\tau) d\tau$$

Define $B_j := B(\vec{\omega}(jh))$. Approximating the integral by the trapezoidal rule one gets:

$$\left(I + \frac{h}{2} B_{j+1}\right) \vec{\omega}((j+1)h) = \left(I - \frac{h}{2} B_j\right) \vec{\omega}(jh) + O(h^3).$$

¹ $\omega^N(x, t) := \sum_{|k_i| \leq N} \omega_k(t) \phi_k(x)$ where the coefficients ω_k are components of $\vec{\omega}$

By noting that $B_{j+1} = B_j + hB(\frac{d\vec{\omega}}{dt}(jh)) + O(h^2)$ we can simplify the above equation compromising the order of the approximation: specifically, approximating B_{j+1} by $B_j + hB(\frac{d\vec{\omega}}{dt}(jh))$ we reduce the order down to $O(h^2)$ (locally); if we simply take B_j we get $O(h)$ -approximation. In what follows we stick to the latter and define \tilde{w}_j as a solution of the linear system:

$$(I + \frac{h}{2}B_j)\tilde{w}_{j+1} = (I - \frac{h}{2}B_j)\tilde{w}_j, \tilde{w}_0 = \vec{\omega}_0. \quad (8)$$

Note that $(I + \frac{h}{2}B_j)$ is invertible as B_j is skew-symmetric and

$$K_j := (I + \frac{h}{2}B_j)^{-1}(I - \frac{h}{2}B_j)$$

is the Caley transform of the skew-symmetric matrix B_j . Hence, K_j is an orthogonal matrix and so $\|\tilde{w}_j\|_{\mathbb{R}^{2N+1}}^2 = \|\tilde{w}_0\|_{\mathbb{R}^{2N+1}}^2$.

For $j = 1, \dots, m-1$ and $jh \leq t < (j+1)h$ we define the following functions: $U^{(m)}(t) := \frac{\tilde{w}_{j+1} + \tilde{w}_j}{2}$, $V^{(m)}(t) = \tilde{w}_j$ and $W^{(m)}(t) = \tilde{w}_j - (t - jh)B(\tilde{w}_j)U^{(m)}(t)$. Since $\|\tilde{w}_j\|_{\mathbb{R}^{2N+1}}^2 = \|\tilde{w}_0\|_{\mathbb{R}^{2N+1}}^2$ it follows that $\|V^{(m)}\|_{L^2(0,T)}, \|U^{(m)}\|_{L^2(0,T)} \leq C_1 < +\infty$ and so $\|W^{(m)}\|_{L^2(0,T)} \leq C_2 < +\infty$. Therefore, the sequences of piecewise constant functions, $\{V^{(m)}\}_{m \in \mathbb{N}}, \{U^{(m)}\}_{m \in \mathbb{N}}$ contain weakly convergent subsequences in $L^2(0,T)$. The same holds true for the sequence $\{W^{(m)}\}_{m \in \mathbb{N}}$. We denote the convergent subsequences by $\{V^{(m_i)}\}, \{U^{(m_i)}\}$ and $\{W^{(m_i)}\}$ respectively and let V^*, U^* and W^* be their limiting functions.

We claim that all the three mentioned sequences converge strongly and $V^* = U^* = W^*$. Indeed, $\frac{dW^{(m_i)}}{dt} = -B(V^{(m_i)}(t))U^{(m_i)}(t)$ and so $\frac{dW^{(m_i)}}{dt}$ is bounded in $L^2(0,T)$. Hence, $\{W^{(m_i)}\}$ weakly converges in $H^1(0,T)$ that implies strong convergence in $L^2(0,T)$. Now, $\|V^{(m_i)} - U^{(m_i)}\|_{L^2(0,T)} \leq h^{\frac{3}{2}}m^{\frac{1}{2}}\|\tilde{w}_0\|_{\mathbb{R}^{2N+1}}^{\frac{C_2}{2}}$ where $C := \sum_{j=1}^{2N+1} \|B(e_j)\|^2$, e_j is j -th canonical basis vector. Hence, by taking

weak limit ($m \rightarrow \infty$) and using weak lower-semicontinuity of L^2 -norm we get: $V^* = U^*$. On the other hand $\|W^{(m_i)} - V^{(m_i)}\|_{L^2(0,T)}^2 \leq \frac{h^3}{3} \sum_{j=1}^m \|B(\tilde{w}_j)U^{(m_i)}(t)\|_{\mathbb{R}^{2N+1}}^2 \leq \frac{h^3}{3} C \|\tilde{w}_0\|_{\mathbb{R}^{2N+1}}^4$. By the same argument we get: $W^* = V^*$. Taking weak limits in $\frac{dW^{(m_i)}}{dt} = -B(V^{(m_i)}(t))U^{(m_i)}(t)$ we find that: $\frac{dW^*}{dt} = -B(W^*)W^*(t)$.

Now, recalling the spectral convergence rate estimate (7) and noting that there exists unique smooth solution of (1) we deduce that any convergent subsequence of $U^{(m)}, V^{(m)}$ and $W^{(m)}$ has the same limit. The latter proves that the entire sequences $U^{(m)}, V^{(m)}$ and $W^{(m)}$ are weakly convergent and share the same limiting function W^* which is the unique solution of (4).

Let us summarize the above results.

Proposition 1: If $f = 0$ then

- (i) (4) has a unique solution $\vec{\omega}$ such that $\|\vec{\omega}(0)\|_{\mathbb{R}^{2N+1}} = \|\vec{\omega}(t)\|_{\mathbb{R}^{2N+1}}$,
- (ii) a sequence of piecewise constant functions $V^{(m)}(t) = \tilde{w}(jh)$, $jh \leq t < (j+1)h$ converges to $\vec{\omega}$ in $L^2(0,T)$ provided $\tilde{w}(jh)$ solves (8) and $h := \frac{T}{m}$, $m \in \mathbb{N}$.

We note that it is not hard to generalize point (ii) of the latter proposition to the case $f \neq 0$. We omit this generalization here for the sake of space.

C. State estimator

Following [6] we introduce the following system of linear Hamiltonian equations:

$$\begin{pmatrix} I - \frac{h}{2}B_j^\top & \frac{h}{2}H^\top RH \\ \frac{h}{2}Q^{-1} & I + \frac{h}{2}B_j \end{pmatrix} \begin{pmatrix} U_{j+1} \\ V_{j+1} \end{pmatrix} = \begin{pmatrix} I + \frac{h}{2}B_j^\top & \frac{h}{2}H^\top RH \\ \frac{h}{2}Q^{-1} & I - \frac{h}{2}B_j \end{pmatrix} \begin{pmatrix} U_j \\ V_j \end{pmatrix}, \quad (9)$$

where $P_j := U_j^{-1}V_j$ for $j > 0$ and $P_0 = S^{-1}$, and $B_j := B(\hat{\omega}_j)$, and $\hat{\omega}_j$ solves the following system

of linear equations:

$$\begin{aligned} & \left(I + \frac{h}{2}B_j + \frac{h}{2}P_{j+1}H^\top RH\right)\hat{\omega}_{j+1} \\ &= \left(I - \frac{h}{2}B_j - \frac{h}{2}P_jH^\top RH\right)\hat{\omega}_j \quad (10) \\ &+ \frac{h}{2} \frac{P_{j+1}H^\top R\vec{y}_{j+1} + P_jH^\top R\vec{y}_j}{2}, \end{aligned}$$

where $H := \{(H_k, \phi_s)_{L^2(\Omega)}\}_{|k_{1,2}|, |s_{1,2}| \leq N}$. By combining the idea of the proof of Proposition 1 with a well-known stabilization effect brought by P_j , the solution of approximated Riccati equation (see [6] for the details), one may prove the following proposition.

Proposition 2: Let U_j, V_j, P_j and $\hat{\omega}_j$ be defined as above and $h := \frac{T}{m}$, $m \in \mathbb{N}$. A sequence of piecewise constant functions $V^{(m)}(t) = V_j$, $U^{(m)}(t) = U_j$, $\hat{\omega}^{(m)}(t) = \hat{\omega}_j$ for $jh \leq t < (j+1)h$ converges to U, V and $\hat{\omega}$ in $L^2(0, T)$. Moreover, U, V and $\hat{\omega}$ represent the unique solution of the following system of equations:

$$\begin{aligned} \frac{d\hat{\omega}}{dt} &= -B(\hat{\omega})\hat{\omega} + PH^\top RH(\vec{y} - H\hat{\omega}), \hat{\omega}(0) = 0, \\ \frac{dU}{dt} &= B^\top(\hat{\omega})U + H^\top RHV, U(0) = I, \\ \frac{dV}{dt} &= Q^{-1}U - B(\hat{\omega})V, V(0) = S^{-1}, P = VU^{-1}. \end{aligned} \quad (11)$$

In fact, the latter proposition presents a continuous version of the minimax filter (equation (11)) and equations (9)-(10) define an approximation for the filter. In the following section we illustrate the convergence properties of this approximation on numerical examples.

IV. NUMERICAL EXPERIMENTS

A. Euler equations

For the divergence-free Euler system, we look for solutions in the space, $\text{span}\{\phi_k(x) := \phi_{k_1}(x)\phi_{k_2}(y)\}_{k_1=0\dots N_x, k_2=0\dots N_y}$, where $\psi_{k_1}(z) = \sin(k_1\pi z/L)$, $L = 2r$ is the length of each side of the spatial domain, and N_x and N_y are the numbers of basis functions in each of the spatial

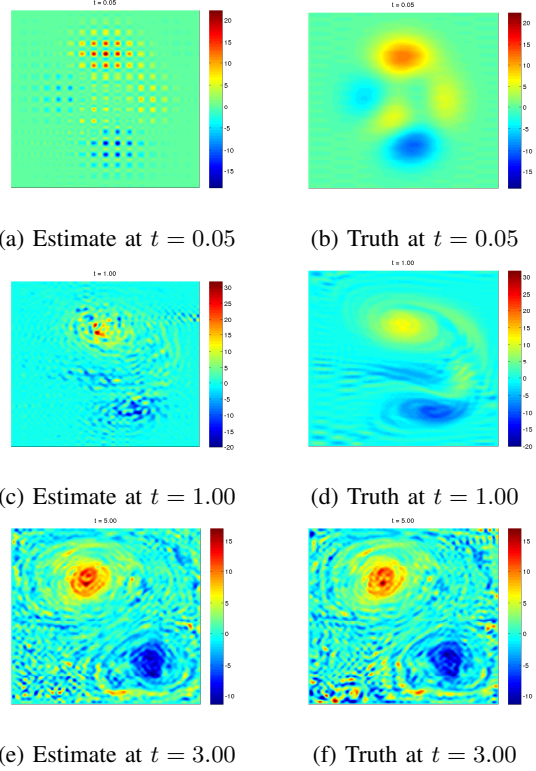
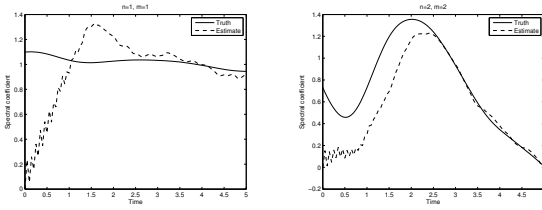
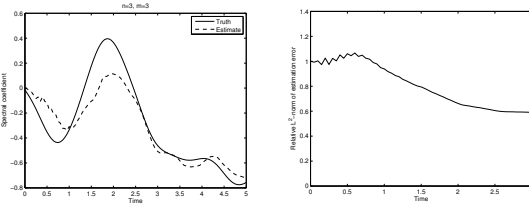


Fig. 1: Estimates and truth for different times

dimensions. The choice of basis satisfies the boundary conditions, $\omega = 0$ on $\partial\Omega$. The corresponding Fourier-Galerkin model (4) is subject to the perturbation vector \vec{f} which has only two non-zero entries, meaning that in effect, we perturb only two modes: one low, and one high frequency mode. For the filter, we first generate observations \vec{y} by running (4) the Euler system forward in timewith initial condition represented by a translation and scaling of Gaussian distributions. The filter is initialized to zero, meaning we assume no knowledge of the initial condition. Observations are taken on an evenly spaced 15×15 grid away from the boundary, where the state is fixed at zero. For both the generation of observations and the filtering, we choose $N_x = N_y = 60$. Figure 1 shows the estimate and truth at different times. The sparsity of the observations is apparent from Figure 1a,



(a) Projection coefficients for $k_1 = k_2 = 1$ (b) Projection coefficients for $k_1 = k_2 = 2$



(c) Projection coefficients for $k_1 = k_2 = 3$ (d) Relative L^2 -error of the estimate

which is from an early point in the estimation. In Figure 1c, we see that by $t = 1.00$, the estimate does still not fully mimic the truth, but that the flow is being captured. In Figure 1e, the estimate appears to capture the truth quite well. Figures 2a - 2c show the estimated and true projection coefficients for some of the low wave numbers.

B. Lighthill-Whitham-Richards (LWR) model

In this section we apply the above method to scalar conservation laws. Recall from [9] that the standard equilibrium traffic-flow model, LWR model consists of a scalar conservation law,

$$\partial_t u(x, t) + \partial_x f(u(x, t)) = 0, \quad (12)$$

with initial data $u_0(x) = u(x, 0)$ where $u : \mathbb{R} \times \mathbb{R}_+ \rightarrow \mathbb{R}$ is the traffic density, $x \in \mathbb{R}$ and $t \in \mathbb{R}_+$ are the independent variables, space and time respectively, and $f : \mathbb{R} \rightarrow \mathbb{R}$ is the flux function. A typical flux function is $f(u) = uV_m \left(1 - \frac{u}{u_m}\right)$ where the constants, V_m and u_m , are the maximum speed and the maximum density respectively. We impose periodic boundary conditions on the interval $(0, 2\pi)$. Unlike the Euler equation presented above,

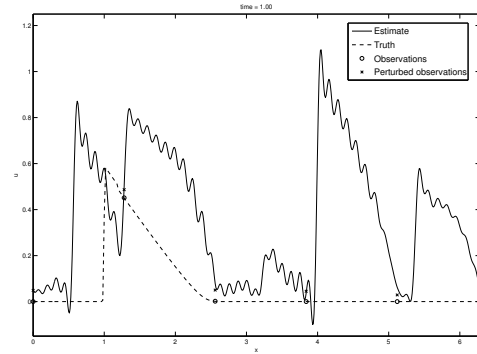


Fig. 3: True traffic state versus estimate at $t=1$

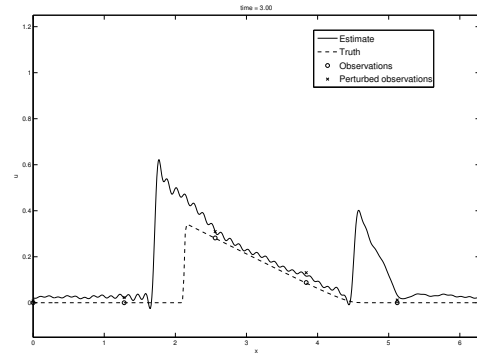


Fig. 4: True traffic state versus estimate at $t=3$

this model develops shock discontinuities even subject to periodic boundary conditions and smooth initial condition. The filter has been applied to the Fourier-Galerkin model² which has been used to generate observations. The filter has been initialized to 0. The estimation results are presented on the figures 3-5. We refer the reader to [9] for the further details.

C. St Venant equations

This final example shows that the proposed state estimator may handle systems of conservation laws

²The model had artificial viscosity term activated on higher order modes to allow for correct shock tracking

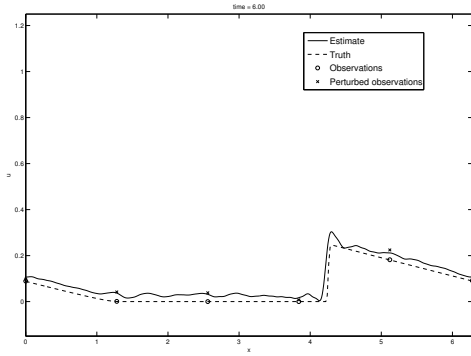


Fig. 5: True traffic state versus estimate at $t=6$

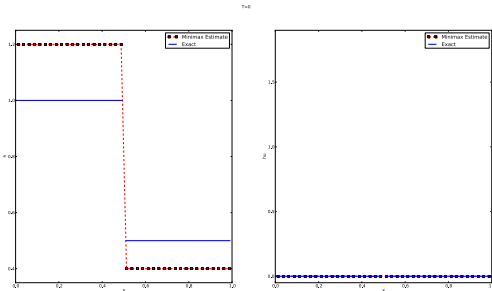


Fig. 6: Initial conditions for h , hu and the estimate

with non-periodic boundary conditions. The standard equilibrium flood model consists of a system of scalar conservation laws:

$$\begin{aligned} \partial_t h + \partial_x(hu) &= 0, \\ \partial_t(hu) + \partial_x(hu^2 + \frac{gh^2}{2}) &= 0 \end{aligned} \quad (13)$$

with boundary conditions $u(0, t) = u_l(t)$ and $h(0, t) = h_l(t)$ on $(0, 1)$, where h is the fluid depth, u is the averaged velocity and g is the gravitational constant. The Discontinuous Galerkin method has been applied to the above equation to generate observations. There was no perturbation, so $\vec{f} = 0$. The initial conditions for the model and filter are presented at Figure 6. The estimation results are presented on the figures 7-8. We refer the reader to [11] for the further details.

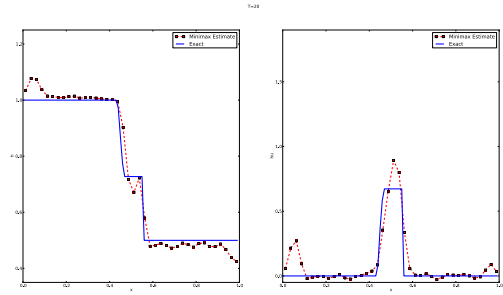


Fig. 7: h , hu and the estimate after 20 time steps

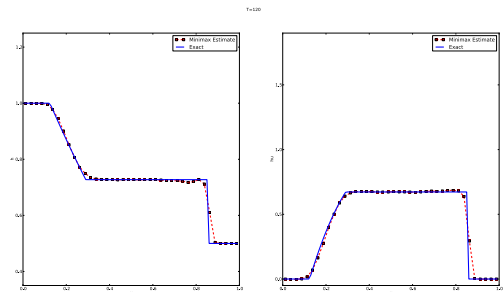


Fig. 8: h , hu and the estimate after 120 time steps

V. CONCLUSION

The paper presents the discrete and continuous versions of the minimax state estimator for Euler equations. The estimator is derived for a Fourier-Galerkin model which approximates smooth solutions of the Euler equation with spectral convergence rate. A very curious topic for the future research is to develop the idea of [9] for weak solutions of Euler equations, that is to combine the presented state estimation approach and vanishing viscosity method [1] to design a state estimator for L^∞ solutions of Euler equations in vorticity-stream formulation. We stress that the presented method and convergence results apply to Navier-Stokes equations in dimension 2 without major modifications.

REFERENCES

- [1] C. Bardos and E. Tadmor. Stability and spectral convergence of fourier method for nonlinear problems: on the shortcomings of the 2/3 de-aliasing method. *Numerische Mathematik*, 129(4), 2015.
- [2] C. Bardos and E. Titi. Euler equations of incompressible ideal fluids. *Uspekhi Matematicheskikh Nauk*, 62(3):5–46, 2007.
- [3] Claude Bardos and Olivier Pironneau. Data assimilation for conservation laws. *Methods and Applications of Analysis*, 12(2):103–134, 06 2005.
- [4] S. Blandin, A. Couque, A. Bayen, and D. Work. On sequential data assimilation for scalar macroscopic traffic flow models. *Physica D*, 2012.
- [5] M. Demetriou and H. Banks. Adaptive parameter estimation of hyperbolic distributed parameter systems: Non-symmetric damping and slowly time varying systems. *ESAIM: Control, Optimisation and Calculus of Variations*, 3:133–162, 1998.
- [6] J. Frank and S. Zhuk. Symplectic möbius integrators for lq optimal control problems. In *Proc. IEEE Conference on Decision and Control*, 2014.
- [7] A. Majda and A. Bertozzi. *Vorticity and incompressible flow*. Cambridge Univ. Press, 2002.
- [8] V. Mallet and S. Zhuk. Reduced minimax filtering by means of differential-algebraic equations. In *5th Int. Conf. on Physics and Control*, 2011. lib.physcon.ru.
- [9] T. Tchraïkian and S. Zhuk. A macroscopic traffic data assimilation framework based on Fourier-Galerkin method and minimax estimation. *IEEE Transactions on Intelligent Transportation Systems*, (99):1–13, 2014. special issue.
- [10] R. Temam. *Navier-Stokes equations: Theory and Numerical Analysis*. AMS Chelsea Publishing, 2001.
- [11] S. Tirupathi, S. Zhuk, T. Tchraïkian, and S. McKenna. Data assimilation for 1d shallow water equations: a minimax approach. *in preparation*, 2015.
- [12] V. Yudovich. Non-stationary flow of an incompressible liquid. *Zh. Vychisl. Mat. Mat. Fiz.*, pages 1032–1066, 1963.
- [13] S. Zhuk. Kalman duality principle for a class of ill-posed minimax control problems with linear differential-algebraic constraints. *Applied Mathematics and Optimization*, 68(2):289–309, 2013.
- [14] S. Zhuk. Minimax projection method for linear evolution equations. In *Proc. IEEE Conference on Decision and Control*, ieeexplore.ieee.org, 2013.
- [15] S. Zhuk, J. Frank, I. Herlin, and R. Shorten. Data assimilation for linear parabolic equations: minimax projection method. *SIAM J. Sci. Comp.*, 2015. to appear.